

Catalytic Aziridination of Styrene with Copper Complexes of Substituted 3,7-Diazabicyclo[3.3.1]nonanones

Peter Comba,^{*[a]} Michael Merz,^[a] and Hans Pritzkow^[a]

Keywords: Copper / N ligands / Catalysis

The copper(II) complexes of five bispidine-type ligands {3,7-diazabicyclo[3.3.1]nonanone; three tetradentate ligands with 2-pyridyl (L^1), 6-methyl-2-pyridyl (L^2) or 2-imidazolyl-3-methyl (L^3) substituents in 2,4-positions; two pentadentate derivatives of L^1 with an additional 2-methylpyridine substituent at N3 (L^4) or N7 (L^5)} have, with one co-ligand (Cl^-), a ligand-enforced square pyramidal ($L^{1,2,3}$) or octahedral ($L^{4,5}$) geometry. The main structural properties of three of the five $[Cu(L)(Cl)]^+$ complexes ($L^{1,2,3}$) are very similar, with $Cu-N3 < Cu-N7$ and $Cu-Cl \approx 2.25 \text{ \AA}$ (*trans* to N3); with L^2 $Cu-N3 \approx Cu-N7$ and $Cu-Cl = 2.22 \text{ \AA}$ (*trans* to N7); with L^5 $Cu-N3 < Cu-N7$ and $Cu-Cl = 2.72 \text{ \AA}$ (*trans* to N7). These structural patterns lead to considerable differences in ligand field and electrochemical properties (range of E° of approx. 500mV), and the reactivities of the copper(II) complexes as aziridin-

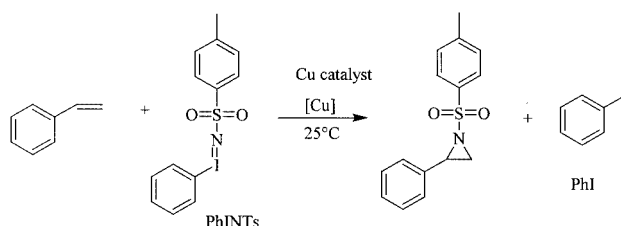
ation catalysts (styrene, PhINTs, CH_3CN) are strikingly different. While the complex with L^2 is very efficient, the activities of those with L^1 and L^3 are reduced to approx. 50% and 30%, respectively, and those with L^4 and L^5 are inactive. The fact that the maximum TON (maximum turnover number) of $Cu^{II}L^2$ (19) is much smaller than the maximum TON of Cu^IL^2 (47) suggests that in the active form the catalysts are in the Cu^I oxidation state, and that the differences in reduction potentials are of major importance for catalysis. The result that $CuL^{4,5}$ have no activity in the Cu^{II} state and only a small activity in the reduced form indicates that, apart from the reduction potentials, steric effects might also be of importance.

(© Wiley-VCH Verlag GmbH & Co. KGaA, 69451 Weinheim, Germany, 2003)

Introduction

Aziridines, the nitrogen analogues of epoxides, are attractive intermediates in organic synthesis,^[1,2] and various aziridine-containing natural products have cytotoxic properties.^[3,4] Their synthesis, mediated by copper powder, has been known for many years,^[5] and transition metal-catalyzed procedures have recently attracted much attention (Scheme 1).^[6] Since their discovery^[7–9] copper-catalyzed processes have been studied extensively, and various enantioselective catalysts have been developed.^[10–12] PhINTs { $[N-(p\text{-toluenesulfonyl})\text{imino}]$ phenyliodinane} is the most frequently used nitrene source in copper-catalyzed aziridination reactions, but others have also been described.^[13–15] An interesting observation is that both copper(I) and copper(II) complexes have been found to be active catalysts. Two possible general mechanisms have been discussed, one which involves the copper complexes as Lewis acid catalysts (activation of the coordinated iodine without electron transfer) and, in analogy to cyclopropanation, a process with a discrete copper-nitrene intermediate (electron transfer).^[11,12] Recent experimental evidence^[11,16,17] and theoretical studies^[17] indicate that there is a discrete nitrene inter-

mediate, and that the copper(I) complexes are the active catalysts, leading to a copper(I)-nitrene or a copper(III)-imido species; the copper(II) pre-catalysts may enter the catalytic cycle via reduction by PhINTs to the corresponding copper(I) complexes.^[17] Interesting questions related to this latter mechanism are the electronic structure, spin state and copper oxidation state of the catalytically active intermediate, i.e., whether it is best formulated as a copper(I)-nitrene or a copper(III)-imido species, and the coordination mode of the nitrene donor, derived from PhINTs, which generally is formulated as a monodentate ligand and recently has been proposed to coordinate as a bidentate with the sulfonyl oxygen atom being an additional donor.^[17]



Scheme 1

Copper(II)-catalyzed reactions are of particular interest since, in contrast to copper(I), the catalysts are air-stable. A

^[a] Universität Heidelberg, Anorganisch-Chemisches Institut, Im Neuenheimer Feld 270, 69120 Heidelberg
Fax: (internat.) + 49-(0)6226-546617
E-mail: comba@akcomba.oci.uni-heidelberg.de

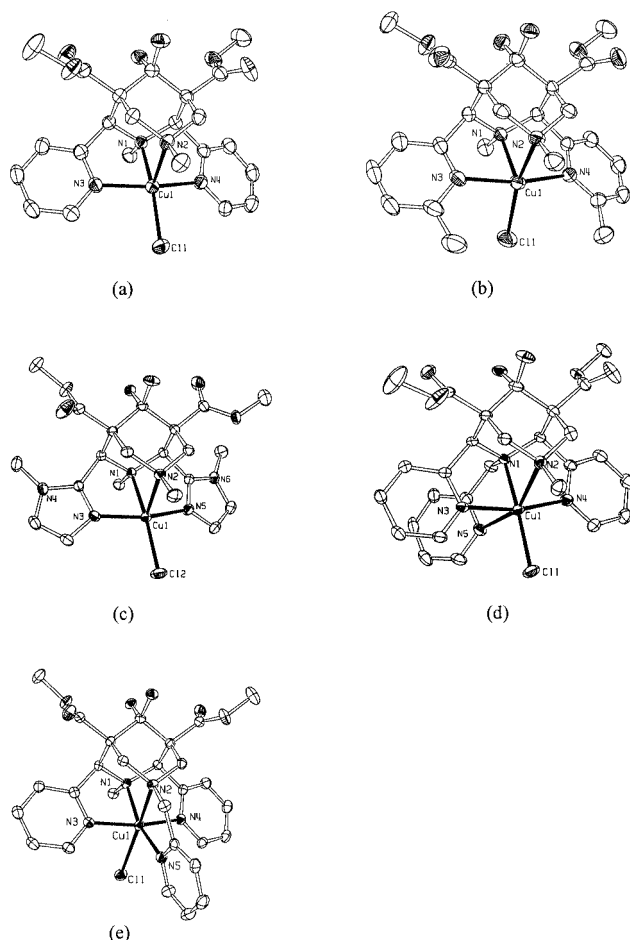


Figure 1. ORTEP^[34] plots of (a) $[\text{Cu}(\text{L}^1)(\text{Cl})]^+$,^[19] (b) $[\text{Cu}(\text{L}^2)(\text{Cl})]^+$,^[20] (c) $[\text{Cu}(\text{L}^3)(\text{Cl})]^+$, (d) $[\text{Cu}(\text{L}^4)(\text{Cl})]^+$, (e) $[\text{Cu}(\text{L}^5)(\text{Cl})]^+$

cal considerations^[21] and translates to generally strongly bound and highly activated substrates (peroxide, catecholate)^[22–25] and an unprecedented high stability constant for chloride.^[29] The main structural features of $[\text{Cu}(\text{L}^3)(\text{Cl})]^+$ and $[\text{Cu}(\text{L}^4)(\text{Cl})]^+$ are, as expected, similar to those of $[\text{Cu}(\text{L}^1)(\text{Cl})]^+$ (see Cu–N1, Cu–N2, Cu–Cl, Figure 1, Table 1). The structural differences of the aromatic five- vs. six-membered ring (L^1 vs. L^3) and the small differences in donor strength between imidazole and pyridine (strong σ -donors, $\text{p}K_{\text{a}}(\text{pyridine}) = 5.3$, $\text{p}K_{\text{a}}(\text{imidazol}) = 7.1$, weak π -acids) lead only to minor structural variations. The addition of a third pyridine donor *trans* to N2 (L^4 , additional pyridine donor in the “Jahn–Teller” axis, 2.5 vs. 2.0 Å) also leads to only small over-all structural changes (Cu–Cl = 2.25 Å, similar to $\text{L}^{1,3}$).

More important and interesting are the structural changes enforced by L^2 (α -methyl substitution of the pyridine donors, steric crowding) and L^5 (ligand-enforced coordination of the substrate in the “Jahn–Teller” axis, *trans* to N2). In the latter case (L^5) the structural features are obvious and as expected: the distance to the third pyridine donor is similar to that of the other two (Cu–N3 \approx Cu–N4 \approx Cu–N5, note the differences to the structure with L^4), and Cu–Cl = 2.72 Å (in contrast to all the other complexes discussed here, but similar to the usual CuN_5Cl^+ (and CuN_4Cl^+) chromophores, see above).

The most interesting structure, however, is probably that of the complex with L^2 . The methyl substitution enforces the coordination of bulky co-ligands (substrates) such as Cl^- *trans* to N2 (note that the sterically less demanding NCCCH_3 donor is coordinated *trans* to N1^[23]). The resulting structure is best described as square pyramidal with the two pyridine donors, Cl^- and N2 in-plane, and N1 as the axial donor (see Figure 2). The main structural differences be-

Table 1. Selected bond lengths (Å) and angles (deg) of the molecular cations of the copper(II) complexes

Bond lengths [Å]	$[\text{Cu}(\text{L}^1)(\text{Cl})]^+$	$[\text{Cu}(\text{L}^2)(\text{Cl})]^+$	$[\text{Cu}(\text{L}^3)(\text{Cl})]^+$	$[\text{Cu}(\text{L}^4)(\text{Cl})]^+$	$[\text{Cu}(\text{L}^5)(\text{Cl})]^+$
Cu–N1	2.042(3)	2.147(3)	2.115(2)	2.070(2)	2.036(2)
Cu–N2	2.272(3)	2.120(3)	2.316(2)	2.478(2)	2.368(2)
Cu–N3	2.020(3)	2.061(3)	1.967(2)	2.011(2)	2.028(2)
Cu–N4	2.024(3)	2.064(3)	1.971(2) ^[a]	1.987(2)	2.029(2)
Cu–N5	–	–	–	2.544(2)	2.029(2)
Cu–Cl	2.232(1)	2.221(2)	2.2285(6)	2.2546(8)	2.717(6)
N1...N2	2.921	2.930	2.917	2.931	2.915
N3...N4	3.971	4.084	3.869 ^[a]	3.965	3.995
Valence angles [°]					
N1–Cu–N2	85.02(9)	86.71(12)	82.20(6)	79.70(8)	82.53(6)
N1–Cu–N3	81.25(10)	81.63(13)	80.58(7)	83.62(9)	81.39(7)
N1–Cu–N4	81.15(10)	82.37(13)	80.51(7) ^[a]	81.74(10)	80.94(7)
N1–Cu–N5	–	–	–	77.95(10)	160.82(7)
N2–Cu–N3	95.95(10)	91.18(13)	91.54(7)	89.39(9)	88.32(6)
N2–Cu–N4	95.35(10)	90.26(13)	95.77(7) ^[a]	88.27(9)	98.43(6)
N3–Cu–N4	158.13(10)	163.82(13)	158.58(7) ^[a]	165.36(10)	160.07(7)
N2–Cu–N5	–	–	–	155.11(10)	79.27(7)

^[a] For $[\text{Cu}(\text{L}^3)(\text{Cl})]^+$ N4 in this table corresponds to the crystallographic label N5 (see Figure 1).

tween $[\text{Cu}(\text{L}^1)(\text{Cl})]^+$ and $[\text{Cu}(\text{L}^2)(\text{Cl})]^+$ are then (i) a rotation of the pyridine rings out of the xy plane with the methylated ligand L^2 ; this leads to a destabilization of the entire complex and of the Cu–Cl bond,^[21] and (ii) a quenching of the Jahn–Teller-type electronic stabilization due to steric constraints from the bispidine backbone ($\text{Cu–N1} \approx \text{Cu–N2}$), again leading to destabilization.^[26] The stability constant with L^2 is not yet available. However, it is known^[30] that differences in the potential of copper(II/I) couples are strongly correlated with the complex stabilities of the corresponding copper(II) complexes. The difference in the reduction potential between $\text{Cu}^{\text{II}}\text{L}^1$ and $\text{Cu}^{\text{II}}\text{L}^2$ of approx. 300 mV (see below) leads to a difference in total energy of approx. 30 $\text{kJ}\cdot\text{mol}^{-1}$. The computed energy difference (DFT)^[21] is approx. 20 $\text{kJ}\cdot\text{mol}^{-1}$, and some of this difference (approx. 10 $\text{kJ}\cdot\text{mol}^{-1}$) might be due to the quenching of the Jahn–Teller effect, which was not included in the DFT study (model compound with monodentate ligands).^[21] Note, however, that some of these data refer to gas phase calculations and that the co-ligand is not the same in all the studies referred to, i.e., the quoted energies have to be considered with care. Interestingly, the two Cu–Cl bond lengths in the structures with L^1 and L^2 are similar (see Table 2), supporting the interpretation of the structure as square pyramidal with an in-plane Cu–Cl bond, and the short bond is probably also due to less repulsion between Cl^- and the ligand backbone of L^2 (see Figure 2). The theoretically expected decrease in bonding energy^[21] is paralleled by a decrease in Cu–Cl stability by an experimentally observed factor of approx. 2.^[29]

Also relevant for the aziridination catalysis are the corresponding copper(I) structures. A number of solid state structures have been reported,^[23,25,27] and these are similar to the corresponding copper(II) structures. An interesting

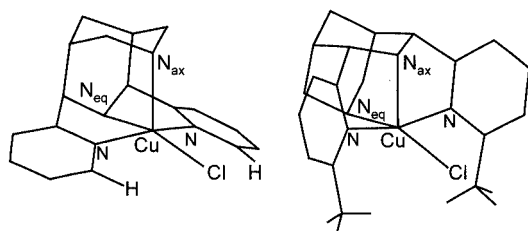


Figure 2. Plots of the crystal structures of $[\text{Cu}(\text{L}^1)(\text{Cl})]^+$ ^[22] and $[\text{Cu}(\text{L}^2)(\text{Cl})]^+$,^[23] visualizing the square pyramidal structure of $[\text{Cu}(\text{L}^2)(\text{Cl})]^+$

feature is that with L^1 four- and five-coordinated complexes are known, which differ by one of the pyridine donors (N3 or N4) either being coordinated or not.^[23] The dynamics in solution are not yet fully understood but the structural data and a qualitative interpretation of the solution NMR spectra suggest that an equilibrium which also involves a reduced coordination number species is feasible.

Spectroscopy and Electrochemistry: Electronic spectra of the copper(II) complexes of the five bispidine ligands L^{1-5} have been recorded as the chloro complexes (chloride salts) and with a coordinated solvent molecule (tetrafluoroborate salts), each in two different solvents (acetonitrile and methanol), see Table 2. The data of the chloro complexes indicate that chloride remains coordinated, i.e., the spectra are close to identical in the two solvents and different from the spectra of the corresponding tetrafluoroborate salts, which differ for each solvent. This was expected from the strong bonds (see above and ref.^[21]), the high stability constants,^[29] and is also supported by conductometric experiments with $\text{L}^{1,2}$.^[25] Worth noting is the strongly different chromophore of the copper(II) complexes with L^4 (generally very weak ligand field), which might be due to the considerable angular distortion of the hexacoordinate complex ($\text{N2–Cu–N5} = 155^\circ$) and/or subtle changes in π -bonding. The solvent-dependent shift of the dd transitions of the copper(II) complexes with L^2 is much larger than it is for the other complexes and suggests some significant structural changes. For the co-ligands Cl^- and NCCH_3 this was expected, i.e., the former coordinates *trans* to N2, the latter *trans* to N1.^[23]

Preliminary EPR spectroscopic data are also included in Table 2. The expected trends (g vs. ligand field strength, g vs. A) are observed but the differences are not significant enough, and the lack of resolution in the ligand field spectra, as well as the lack of a thorough assignment do not warrant further interpretation at present. An interesting feature is that, in the EPR spectrum of $[\text{Cu}(\text{L}^1)\text{Cl}]^{2+}$ (in MeOH or DMF/ H_2O , frozen solution), there is a well resolved fine-structure in the g_{xy} region of the spectrum; a less well resolved but clearly observable fine-structure is also apparent in the g_z region, and in the g_{xy} region of $[\text{Cu}(\text{L}^4)\text{Cl}]^{2+}$. A more detailed interpretation of these and other spectroscopic features will be given elsewhere.

The reduction potentials are also given in Table 2. These are a measure of the stabilities of the copper(II) complexes

Table 2. Spectroscopic and electrochemical properties of the copper(II) complexes of L^{1-5}

Compound	dd Transitions (nm)				EPR ($X = \text{Cl}^-$ ^[a] / $X = \text{CH}_3\text{CN}$ ^[b])			E° ($X = \text{CH}_3\text{CN}$) ^[a] (mV vs. Ag/AgNO ₃)
	$X = \text{Cl}^-$ ^[a]	$X = \text{MeOH}$ ^[b]	$X = \text{CH}_3\text{CN}$ ^[b]	$X = \text{H}_2\text{O}$ ^[b]	g_{\parallel}	g_{\perp}	A_{\parallel}	
$[\text{Cu}(\text{L}^1)(\text{X})]^{n+}$	650 (sh, 700)	660	630	653	2.225/2.245	2.034/2.072	176/172	–417
$[\text{Cu}(\text{L}^2)(\text{X})]^{n+}$	625 (sh, 740)	785 (sh, 830)	700	625 (sh, 740)	2.245/2.245	2.065/2.085	160/165	–98
$[\text{Cu}(\text{L}^3)(\text{X})]^{n+}$	640 (sh, 690)	665	650	–	2.230/2.250	2.070/2.070	165/168	–440
$[\text{Cu}(\text{L}^4)(\text{X})]^{n+}$	720 (sh, 780)	705	665	–	2.255/2.250	2.06/2.08	160/165	–489
$[\text{Cu}(\text{L}^5)(\text{X})]^{n+}$	640	625	625	–	2.250/2.230	2.060/2.075	170/175	–603

^[a] Cl^- salts; identical spectra in CH_3CN , MeOH (and H_2O). ^[b] BF_4^- salts

(see above).^[30] As expected from the structural data (see above) the electrochemically deduced stabilities of the copper(II) complexes of L^{1,3,4} (coordinated NCCH₃) are similar ($-489 \text{ mV} < E^\circ < -417 \text{ mV}$). That of the complex with L⁵ is significantly larger ($E^\circ = -603 \text{ mV}$; pentadentate ligand; in L⁴ the third pyridine donor is only weakly coordinated and leads to a significant distortion of the chromophore, see spectroscopic data). The difference in E° between the complexes of L¹ and L⁴ suggests that in solution the latter remains hexacoordinate. The reduction potential of the complex with L² is considerably smaller ($E^\circ = -98 \text{ mV}$); i.e., the stability of the copper(II) complex is significantly smaller. Note again that, in CH₃CN, the co-ligand with L² is coordinated *trans* to N1, while other donors (specifically PhINTs) are expected to coordinate *trans* to N2.

Aziridination Catalysis: The efficiency of the aziridination catalytic reactivity of the copper(II) and copper(I) complexes of L¹⁻⁵ are summarized in Table 3. Note that the aziridines were isolated and their yield determined by weight (see Exp. Sect.). This might lead to a loss of product of up to approx. 5%. The reaction time was not optimized but it appears that the reactions with L² and those with copper(I) catalysts are considerably faster than the others.

In a first set of experiments the copper(II) catalysts of L¹⁻⁵ were tested with standard conditions (entries 1,2,5,6,8).^[20] Under these conditions, the pentadentate ligands L^{4,5} do not lead to active copper(II) pre-catalysts, and ligands L^{1,3} lead to catalytic systems of similar activities to those observed recently with other tetradentate ligand systems with two tertiary amine and two pyridine donors.^[20] An interesting feature is that the activity of the copper(II) catalyst with methyl-substituted pyridine donors (L²) is enhanced by a factor of at least 2. In a second series of experiments the maximum turnover number (TON) of the most active copper(II) catalyst (L²) was evaluated (entry 3). A third series of experiments was done to compare the performance of the catalytic systems with copper in the oxidation states (II) and (I) (entries 4,7,9). It appears that the copper(I) forms are generally more efficient. This is supported by the observation that the TONs of the copper(II) systems with the tetradentate ligands L¹⁻³ (entries 1,2,5) are qualitatively correlated to the corresponding reduction potentials (Table 2). The fact that ligands L^{4,5} do not lead

to active copper(II) pre-catalysts indicates that the ease of reducing the pre-catalysts is not the only property related to the catalytic activity (the reduction potential of Cu^{II}(L⁴)X is not much different from those with ligands L^{1,3}). Therefore, another important factor might be that the inner-sphere reduction by PhINTs (as proposed in the literature^[17]) is, for steric reasons, not possible with the pentadentate ligands. This is supported by the fact that the copper(I) complexes with L^{4,5} show some catalytic activity, but this is marginal.

Based on the current data we assume that electronic and steric effects are both responsible for the observed differences in reactivity. Based on the proposal that the copper(II) pre-catalysts enter the catalytic cycle after reduction by PhINTs to the corresponding copper(I) complexes,^[17] the destabilization of the oxidized form by L² might be an important driving force for the higher activity (note again here the ambiguity of the site of coordination of substrates to the complex with L²). PhINTs is a sterically demanding donor, and this is true for a terminal or a chelated copper(I)-nitrene or copper(III)-imido species (with the sulfonyl oxygen atom also coordinated^[17]). Therefore, it is not unexpected that its rate-determining formation with the pentadentate ligand L⁴ is unfavorable. With L⁵, coordination of the substrate to copper(II) is along the Jahn–Teller axis and probably does not lead to a stable interaction, also, this redox potential is extremely negative. Significant differences in steric crowding between the copper-L^{1,2} fragments emerge from Figure 2, the two square pyramidal chromophores are very similar but the L¹ substrate coordination (Cl⁻ in Figure 2) is hindered by the α -CH groups of the pyridine donors; the corresponding methyl groups are not sterically efficient in L². The differences in reactivity between L¹ and L³ (the repulsion due to the α -CH groups in L³ is, for geometric reasons, reduced) indicate that electronic factors (reduction potentials) are also of importance in this case.

Conclusion

Subtle changes on the bispidine backbone have been shown to lead to strikingly different structural and electronic properties of the corresponding copper(II) complexes, and these are transferred to strong differences in the activi-

Table 3. Results of the catalytic aziridination of styrene in CH₃CN (for detailed conditions see text)

Entry	Catalyst	[PhINTs] (mol)	[Catalyst] (mol %)	Yield (%)	TON
1	[Cu ^{II} (L ¹)](BF ₄) ₂	0.4	5	41	9 ± 1
2	[Cu ^{II} (L ²)](BF ₄) ₂	0.4	5	94	19 ± 1
3	[Cu ^{II} (L ²)](BF ₄) ₂	0.6	3.5	67	19 ± 1
4	[Cu ^I (L ²)](BF ₄)	0.9	1.7	80	47 ± 2
5	[Cu ^{II} (L ³)](BF ₄) ₂	0.4	5	29	6 ± 0.5
6	[Cu ^{II} (L ⁴)](BF ₄) ₂	0.4	5	0	0
7	[Cu ^I (L ⁴)](BF ₄)	0.4	1.7	7	7.5 ± 1
8	[Cu ^{II} (L ⁵)](BF ₄) ₂	0.4	5	0	0
9	[Cu ^I (L ⁵)](BF ₄)	0.4	1.7	6	5.5 ± 1

ties of these complexes as aziridination catalysts. It appears that the differences in catalytic activities are due to steric effects and to the destabilization of the copper(II) oxidation state. Bond breaking to one of the pyridine donors in the copper(I) state might facilitate the formation of the copper(I)-nitrene intermediate, and this type of dynamic process with bispidine ligands has been described before.^[23] Further ligand modifications might shed more light on the relative importance of all these factors and lead to more efficient catalytic systems.

Experimental Section

Measurements and Materials: Chemicals for the syntheses and solvents were of the highest degree of purity and used without further purification. The piperidone precursors pL¹ for L^{1,2,5}, the ligands L¹, L², and the corresponding copper(II) complexes (Cl⁻, BF₄⁻ salts) were prepared using published procedures (see Scheme 1).^[23]

IR spectra (KBr pellets) were measured with a Perkin–Elmer 16C FT-IR instrument. NMR spectra were recorded with a Bruker AS 300 spectrometer (¹H, 300.13 MHz; ¹³C, 75.47 MHz); chemical shifts (δ, ppm) are relative to TMS or solvent. Electronic absorption spectra were measured from solutions (approx. 10⁻³ M, CH₃CN), using 1-cm quartz cells, on a Varian Cary 1E instrument. EPR spectra were recorded on a Bruker ELEXSYS E500 spectrometer as approx. 10⁻³ M frozen solutions (liquid nitrogen temperature MeOH, CH₃CN or DMF/H₂O). XSoPhe, version 1.0.2β, on a Linux workstation was used for the computer simulation of the spectra.^[31,32] Electrochemical measurements (cyclic voltammetry, 10–500 mV/s, 2 × 10⁻³ M complex solutions; 0.1 M tetrabutylammonium hexafluorophosphate in acetonitrile) were obtained from a BAS100B system (data analysis with Digisim) with a glassy carbon working, a Pt-wire auxiliary and a Ag/AgNO₃ reference electrode; the potential of the Fc⁺/Fc couple at a scan rate of 100 mV·s⁻¹ lies at 87 mV with ΔE = 64 mV. Mass spectra were recorded with a Finnigan 8400 spectrometer with a nitrobenzyl alcohol matrix for the FAB spectra. Elemental analyses were obtained from the microanalytical laboratory of the University of Heidelberg.

Ligand Syntheses. Piperidones. pL³: Methylamine (1.9 mL, 22.7 mmol, 40%, in water) and dimethyl acetonedicarboxylate (3.95 g, 22.7 mmol) were added to a cold solution (4 °C) of 1-methylimidazole-2-carbaldehyde (5.0 g, 45.4 mmol) in methanol (40 mL). After stirring at 4 °C for 4 h a yellowish white solid occurred, which was collected by filtration and washed with methanol. Yield 5.63 g (14.4 mmol, 63%) of a white solid. C₁₈H₂₃N₅O₅ (389.4): calcd. C 55.52, H 5.95, N 17.98; found C 55.36, H 5.97, N 17.72. ¹H NMR (300 MHz, CDCl₃): δ = 1.79 (s, 3 H, N–CH₃), 3.70 (s, 6 H, N_{Im}–CH₃), 3.72 (s, 6 H, OCH₃), 4.47 (d, ³J_{H,H} = 11.5 Hz, 2 H, CH), 4.84 (d, ³J_{H,H} = 11.4 Hz, 2 H, CH–Im), 6.85 (d, ³J_{H,H} = 1.1 Hz, 2 H, CH_{Im}), 6.92 (d, ³J_{H,H} = 1.1 Hz, 2 H, CH_{Im}) ppm. ¹³C NMR (75.47 MHz, CDCl₃): δ = 30.1 (Im–CH₃), 32.6 (NCH₃), 52.4 (NCH), 53.7 (OCH₃), 59.6 (CH), 122.0 (CH_{Im}), 127.6 (CH_{Im}), 143.8 (C_{Im}), 168.7 (Ester), 199.4 (C=O) ppm. FAB⁺MS(NBA): m/z = 412.2 [M + Na⁺], 390.2 [MH⁺].

pL⁴: The piperidone precursor for L⁴ {3,5-dimethyl-2,6-dipyridyl-N-[2-(pyridyl)methylene]-4-piperidone-3,5-dicarboxylate} was obtained by a dropwise addition of pyridin-2-aldehyde (9.6 mL, 100 mmol), and then picolylamine (5.1 mL, 50 mmol) to an ice-cold solution of dimethyl acetonedicarboxylate (7.2 mL, 50 mmol)

in MeOH (30 mL). After 5 min the orange solution was stored in a freezer (–18 °C). The crystallized product was collected after several days, washed with cold EtOH, and recrystallized from ethanol; a further crop could be obtained by evaporation of the filtrate. Total yield (recrystallized) 19.3 g (42 mmol, 84%).

Bispidones. L³: An aqueous solution of methylamine (40%, 1.1 mL, 13.0 mmol) and aqueous formaldehyde (37%, 2.1 mL, 26 mmol) were added to a suspension of pL³ (4.84 g, 12.4 mmol) in ethanol (200 mL). The suspension was stirred under reflux for 2 h and a clear yellow solution emerged. The solvent was removed under low pressure and the remaining yellow-white solid was recrystallized from ethanol. Yield 3.57 g (8 mmol, 65.2%) of a white solid. C₂₁H₂₈N₆O₅ (444.5): calcd. C 56.75, H 6.35, N 18.90; found C 56.56, H 6.48, N 18.48. ¹H NMR (300.13 MHz, CDCl₃): δ = 1.67 (s, 3 H, NCH₃), 2.49 (s, 3 H, NCH₃), 3.62 (s, 6 H, OCH₃), 3.72 (s, 6 H, N_{Im}–CH₃), 3.73 (d, ²J_{H,H} = 13.9 Hz, 2 H, N–CH₂–), 4.03 (s, 2 H, NCH), 4.63 (d, ²J_{H,H} = 11.7 Hz, 2 H, N–CH₂–), 6.76 (s, 2 H, Im–H), 6.96 (s, 2 H, Im–H) ppm. ¹³C NMR (75.47 MHz, CDCl₃): δ = 32.7 (NCH₃), 37.0 (NCH₃), 45.2 (NCH₂), 52.3 (OCH₃), 59.5 (C_{q,Alkyl}), 63.6 (NCH), 120.9 (Ar–C), 127.0 (Ar–C), 143.9 (Ar–C), 169.9 (ester), 202.0 (C=O) ppm.

L⁴: Aqueous methylamine (40%, 4.8 mL, 56.7 mmol) and formaldehyde (37%, 9.2 mL, 113.4 mmol) were added to a suspension of pL⁴ (21.79 g, 47.3 mmol) in ethanol (250 mL). The suspension was stirred under reflux for 3 h, and a deep-brown solution occurred. The solvent was removed under low pressure and the remaining brown-green solid was recrystallized from ethanol. Yield 6.58 g (12.7 mmol, 27.5%) of a white solid. C₂₈H₂₉N₅O₅ (515.6): calcd. C 65.23, H 5.67, N 13.58; found C 64.86, H 5.60, N 13.41. ¹H NMR (300 MHz, CDCl₃): δ = 2.20 (s, 3 H, N–CH₃), 2.56 (d, ²J_{H,H} = 11.8 Hz, 2 H, –CH₂–), 2.98 (d, ²J_{H,H} = 11.8 Hz, 2 H, –CH₂–), 3.72 (s, 8 H, OCH₃ + CH₂–Py), 5.42 (s, 2 H, CH–Py), 6.76 (d, ³J_{H,H} = 7.7 Hz, 1 H, Py–H), 6.97 (t, ³J_{H,H} = 5.7 Hz, 1 H, Py–H), 7.13 (t, ³J_{H,H} = 6.0 Hz, 2 H, Py–H), 7.38 (t, ³J_{H,H} = 7.6 Hz, 2 H, Py–H), 7.68 (t, ³J_{H,H} = 7.6 Hz, 2 H, Py–H), 8.06 (d, ³J_{H,H} = 7.6 Hz, 1 H, Py–H), 8.43 (d, ³J_{H,H} = 4.6 Hz, 1 H, Py–H), 8.47 (d, ³J_{H,H} = 4.4 Hz, 2 H, Py–H) ppm. ¹³C NMR (75.47 MHz, CDCl₃): δ = 44.3 (N–CH₃), 52.3 (O–CH₃), 57.2 (CH₂–Py), 60.7 (CH₂–N), 62.3 (CH–Py), 70.2 (C_{q,Alkyl}), 121.5, 122.5, 123.7, 124.3, 135.4, 135.7, 148.9 (C_{Ar,C–N}), 149.0 (C_{Ar,C–N}), 156.5 (C_{q,Ar}), 158.8 (C_{q,Ar}), 168.6 (ester), 203.4 (C=O) ppm. FAB⁺MS (Nibeol): m/z = 538.3 [M + Na⁺], 516.3 [MH⁺].

L⁵: 2-(Aminomethyl)pyridine (4.3 g, 39.7 mmol) and aqueous formaldehyde (37%, 6.5 mL, 79.4 mmol) were added to a suspension of pL¹ (12.71 g, 33.1 mmol) in ethanol (200 mL). The suspension was stirred under reflux for 30 min and a clear brown solution occurred. The solvent was removed under low pressure, and the remaining green/brown solid was recrystallized from ethanol. Yield 4.2 g (8.1 mmol, 25.2%) of a white solid. C₂₈H₂₉N₅O₅ (515.6): calcd. C 65.23, H 5.67, N 13.58; found C 64.95, H 5.62, N 13.48. ¹H NMR (300 MHz, CDCl₃): δ = 1.94 (s, 3 H, N–CH₃), 2.68 (d, ²J_{H,H} = 12.1 Hz, 2 H, –CH₂–), 3.14 (d, ²J_{H,H} = 11.9 Hz, 2 H, –CH–), 3.57 (s, 2 H, CH₂–Py), 3.76 (s, 6 H, OCH₃), 4.66 (s, 2 H, CH–Py), 7.09 (t, ³J_{H,H} = 1.5 Hz, 2 H, Py–H), 7.21 (t, ³J_{H,H} = 6.0 Hz, 1 H, Py–H), 7.33 (d, ³J_{H,H} = 7.6 Hz, 1 H, Py–H), 7.50 (t, ³J_{H,H} = 1.7 Hz, 2 H, Py–H), 7.66 (t, ³J_{H,H} = 7.5 Hz, 1 H, Py–H), 7.92 (d, ³J_{H,H} = 7.8 Hz, 2 H, Py–H), 8.45 (d, ³J_{H,H} = 4.0 Hz, 2 H, Py–H), 8.62 (d, ³J_{H,H} = 4.8 Hz, 1 H, Py–H) ppm. ¹³C NMR (75.47 MHz, CDCl₃): δ = 42.9 (N–CH₃), 52.3 (O–CH₃), 58.5 (CH₂–N), 62.1 (CH–Py), 63.3 (CH₂–Py), 73.6 (C_{q,Alkyl}), 122.2, 122.7, 123.6, 124.3, 136.1, 148.9 (C_{Ar,C–N}), 149.3 (C_{Ar,C–N}), 156.7

($C_{q,Ar}$), 158.2 ($C_{q,Ar}$), 168.3 (ester), 203.2 (C=O) ppm. FAB⁺MS (Nibeol): m/z = 538.3 [$M + Na^+$], 516.3 [MH^+].

Syntheses of the Copper(II) Compounds. General Method: A solution of the metal salt (1 mmol) in methanol (1 mL) was added to a solution of the ligand (1 mmol) in acetonitrile (1 mL). The mixture was stirred for 24 h, the solvent was then evaporated to dryness and the resulting solid washed twice with EtOAc, and dried in vacuo. Note that the ϵ values given below, specifically for the BF_4^- salts, are not necessarily of pure compounds, with various coordinated solvent molecules, e.g. OH_2 , OMe, see text.

[Cu(L³)(Cl)]Cl: $C_{21}H_{28}Cl_2CuN_6O_5 \cdot 2H_2O$ (614.97): calcd. C 41.01, H 5.24, N 13.63; found C 41.33, H 5.30, N 13.89. FAB⁺MS (NBA): m/z = 542.1 ([Cu(L³)(Cl)]H⁺), 560.1 ([Cu(L³)(Cl)(H₂O)]H⁺). IR: $\tilde{\nu}$ = 3198 (m, OH), 3096 (w), 2948 (m), 1732 (s), 1540 (w), 1500 (m), 1282 (s), 1272 (s), 1070 (m), 760 cm^{-1} (w). UV/Vis (MeOH): λ (ϵ , $cm^2 \cdot mol^{-1}$) = 638 (96), 279 (2520), 237 nm (2340).

[Cu(L³)(BF₄)₂]: M.p. 181 °C. $C_{21}H_{28}B_2CuF_8N_6O_5 \cdot 2H_2O$ (717.67): calcd. C 35.14, H 4.49, N 11.71; found C 35.15, H 4.94, N 11.15. FAB⁺MS (NBA): m/z = 525.3 ([Cu(L³)(H₂O)]H⁺). $E_{1/2}$ (MeCN) = -440 mV. IR: $\tilde{\nu}$ = 3502 (s), 3400 (s), 3136 (m), 2958 (m), 1728 (s), 1544 (w), 1504 (m), 1452 (m), 1274 (s), 1040 (s), 758 cm^{-1} (m). UV/Vis (MeOH): λ (ϵ , $cm^2 \cdot mol^{-1}$) = 668 (51), 334 (299), 260 (1088), 237 nm (2289).

[Cu(L⁴)(Cl)]Cl: $C_{28}H_{29}Cl_2CuN_5O_5 \cdot H_2O$ (668.03): calcd. C 49.51, H 4.62, N 10.69; found C 49.53, H 4.89, N 11.05. FAB⁺MS (NBA): m/z = 631.2 ([Cu(L⁴)(Cl)(OH₂)]H⁺). IR: $\tilde{\nu}$ = 3376 (s, OH), 3101 (w), 2952 (m), 1724 (s), 1603 (m), 1465 (m), 1423, 1247 (s), 1046 (m), 789 (m), 647 (w), 532 cm^{-1} (w). UV/Vis (MeOH): λ (ϵ , $cm^2 \cdot mol^{-1}$) = 714 (29), 260 nm (3035).

[Cu(L⁴)(BF₄)₂]: $C_{28}H_{29}B_2CuF_8N_5O_5 \cdot 2H_2O$ (788.75): calcd. C 42.64, H 4.22, N 8.88; found C 42.86, H 4.32, N 9.01. $E_{1/2}$ = -489 mV in acetonitrile. IR: $\tilde{\nu}$ = 3386 (s), 3098 (w), 2952 (m), 1726 (s), 1605 (m), 1465 (m), 1423 (m), 1247 (s), 1046 (m), 786 (m), 645 (w), 534 cm^{-1} (w). UV/Vis (MeOH): λ (ϵ , $cm^2 \cdot mol^{-1}$) = 704 (69), 260 nm (3135).

[Cu(L⁵)(Cl)]Cl: $C_{28}H_{29}Cl_2CuN_5O_5 \cdot 2H_2O$ (686.04): calcd. C 49.02, H 4.85, N 10.21; found C 49.06, H 4.81, N 10.27. FAB⁺MS (NBA):

m/z = 631.1 ([Cu(L⁵)(Cl)(H₂O)]H⁺). UV/Vis (MeOH): λ (ϵ , $cm^2 \cdot mol^{-1}$) = 633 (55), 262 (2694), 242 nm (2535).

[Cu(L⁵)(BF₄)₂]: $C_{28}H_{29}B_2CuF_8N_5O_5 \cdot 2H_2O$ (788.75): calcd. C 42.64, H 4.22, N 8.88; found C 42.37, H 4.32, N 8.80. FAB⁺MS (NBA): m/z = 596.3 ([Cu(L⁵)(OH₂)H⁺).

$E_{1/2}$ (MeCN) = -603 mV. IR: $\tilde{\nu}$ = 3444 (s), 3084 (m), 2956 (m), 1730 (s), 1608 (m), 1460 (w), 1438 (m), 1256 (s), 1040 (vs), 764 cm^{-1} (m). UV/Vis (MeOH): λ (ϵ , $cm^2 \cdot mol^{-1}$) = 621 (71), 262 (3483), 247 nm (3337).

Catalysis: The aziridination reactions were performed by stirring mixtures of PhINTs (0.4, 0.5, 0.6 mmol), styrene (1.0 mL) and the copper catalyst (5, 3.5, 1.7 mol% vs. PhINTs) in anhydrous CH_3CN (2.0 mL) under a dry argon atmosphere at 25 °C (the catalyst and PhINTs concentrations were varied to determine the maximum TON, see Results and Discussion; all results reported are averages of at least three experiments). For the studies with the Cu^I catalysts care was taken to do the experiments under strictly anaerobic conditions. After 7 h the green solutions were passed through a short column of neutral alumina to remove the copper species, eluted with EtOAc (20 mL), and the elutes were evaporated to yield oily residues. These crude mixtures were recrystallized with hexane to produce the pure aziridine products. $C_{15}H_{15}NO_2S$ (273.3): calcd. C 65.91, H 5.53, N 5.12; found C 65.84, H 5.56, N 5.14. ¹H NMR (300 MHz, $CDCl_3$): δ = 2.34–2.42 (m, 4 H), 2.98 (d, ³ $J_{H,H}$ = 7.2 Hz, 1 H), 3.77 (dd, ³ $J_{H,H}$ = 4.7, ² $J_{H,H}$ = 2.3 Hz, 1 H), 7.10–7.34 (m, 7 H), 7.88 (d, ³ $J_{H,H}$ = 6.7 Hz, 2 H) ppm.

Crystal Structure Determination: Crystal data and details of the structure determinations are listed in Table 1. Intensity data were collected at low temperature on a Bruker AXS Smart 1000 diffractometer (Mo- K_{α} , λ = 0.71073 Å, ω -scan). Absorption corrections were performed (multiple scans of equivalent reflections, SADABS). The structures were solved by direct methods and refined by full-matrix least-squares against F^2 of all data, using SHELXTL 5.1.^[33]

All non-hydrogen atoms were refined with anisotropic temperature factors. Hydrogen atoms were located in difference Fourier syntheses and refined isotropically. In [Cu(L³)(Cl)]Cl one of the ester groups (at C-5) of the bispidine ligand is disordered. [Cu(L⁴)(Cl)]Cl crystallizes with a disordered acetonitrile molecule.

Table 4. Crystal Data of the copper(II) complexes of L^{3,4,5}

	[Cu(L ³)(Cl)]Cl	[Cu(L ⁴)(Cl)]Cl	[Cu(L ⁵)(Cl)]Cl
Formula	$C_{21}H_{35}Cl_2CuN_6O_9$	$C_{30}H_{34}Cl_2CuN_6O_6$	$C_{28}H_{33}Cl_2CuN_5O_7$
Formula mass	649.99	709.07	686.03
Space group	$P2_1/c$	$P2_1/c$	$P2_1/n$
a , Å	17.9674(11)	12.3631(11)	13.3492(6)
b , Å	11.9389(7)	23.006(2)	15.6044(7)
c , Å	13.0050(8)	11.1856(10)	14.8385(7)
β , deg	97.030(1)	91.465(2)	110.492(1)
V , Å ³	2768.7(3)	3180.5(5)	2895.4(2)
Z	4	4	4
T , K	190(2)	190(2)	173(2)
$\rho_{calcd.}$, $g \cdot cm^{-3}$	1.559	1.481	1.574
μ , mm^{-1}	1.042	0.907	0.995
$R(F_o)$	0.0442	0.0548	0.0351
$wR_2(F_o^2)$	0.1323	0.1595	0.0977
μ , mm^{-1}	1.042	0.907	0.995
$R(F_o)$	0.0442	0.0548	0.0351
$wR_2(F_o^2)$	0.1323	0.1595	0.0977

CCDC 197128–197130 contains the crystallographic data for this paper. This data can be obtained free of charge via www.ccdc.cam.ac.uk/conts/ or from the Cambridge Crystallographic Data Centre, 12 Union Road, Cambridge CB21EZ (Fax: (internat.) +44-1223-336-033; E-mail: depost@ccdc.cam.ac.uk).

Acknowledgments

Generous financial support by the Deutsche Forschungsgemeinschaft (DFG) is gratefully acknowledged. We are grateful to Dr. Lutz Lötzbeyer for measuring the EPR spectra.

- [1] D. Tanner, *Angew. Chem. Int. Ed. Engl.* **1994**, *35*, 599.
- [2] H. C. Kolb, M. G. Finn, K. B. Sharpless, *Angew. Chem. Int. Ed.* **2001**, *40*, 2004.
- [3] S. Shizeki, M. Ohtsuka, K. Irinoda, K. Kukita, K. Nagaoka, T. J. Nakashina, *Antibiot.* **1987**, *40*, 60.
- [4] R. S. Coleman, J.-S. Kong, *J. Am. Chem. Soc.* **1998**, *120*, 3538.
- [5] H. Kwart, A. A. Kahn, *J. Am. Chem. Soc.* **1967**, *89*, 1950.
- [6] P. Müller, *Transition metal-catalyzed nitrene transfer: aziridination and insertion*, vol. 2, JAI Press Inc., **1997**.
- [7] D. A. Evans, M. M. Faul, M. T. Bilodeau, *J. Org. Chem.* **1991**, *56*, 6744.
- [8] D. A. Evans, M. M. Faul, M. T. Bilodeau, B. A. Anderson, D. M. Barnes, *J. Am. Chem. Soc.* **1993**, *115*, 5328.
- [9] D. A. Evans, M. M. Faul, M. T. Bilodeau, *J. Am. Chem. Soc.* **1994**, *116*, 2742.
- [10] Z. Li, K. R. Conser, E. N. Jacobsen, *J. Am. Chem. Soc.* **1993**, *115*, 5326.
- [11] Z. Li, R. W. Quan, E. N. Jacobsen, *J. Am. Chem. Soc.* **1995**, *117*, 5889.
- [12] E. N. Jacobsen, *Aziridiantion*, vol. 2 **1999**.
- [13] T. P. Albone, P. S. Aujnla, P. C. Taylor, S. Challenger, A. M. Derrick, *J. Org. Chem.* **1998**, *63*, 9569.
- [14] P. Dauban, R. H. Dodd, *J. Org. Chem.* **1999**, *64*, 5304.
- [15] A. V. Gontcharov, H. Liu, K. B. Sharpless, *Org. Lett.* **1999**, *1*, 783.
- [16] M. M. Diaz-Requejo, P. J. Perez, M. Brookhart, J. L. Templeton, *Organometallics* **1997**, *16*, 4399.
- [17] P. Brandt, M. J. Södergren, P. G. Andersson, P.-O. Norrby, *J. Am. Chem. Soc.* **2000**, *122*, 8013.
- [18] J. A. Halfen, J. K. Hallman, J. A. Schultz, J. P. Emerson, *Organometallics* **1999**, *18*, 5435.
- [19] J. A. Halfen, D. C. Fox, M. P. Mehn, L. Que, *Inorg. Chem.* **2001**, *40*, 5060.
- [20] J. A. Halfen, J. M. Uhan, D. C. Fox, M. P. Mehn, L. Que, Jr., *Inorg. Chem.* **2000**, *39*, 4913.
- [21] P. Comba, A. Lienke, *Inorg. Chem.* **2001**, *40*, 5206.
- [22] H. Börzel, P. Comba, C. Katsichtis, W. Kiefer, A. Lienke, V. Nagel, H. Pritzkow, *Chem. Eur. J.* **1999**, *5*, 1716.
- [23] H. Börzel, P. Comba, K. S. Hagen, C. Katsichtis, H. Pritzkow, *Chem. Eur. J.* **2000**, *6*, 914.
- [24] H. Börzel, P. Comba, H. Pritzkow, *Chem. Commun.* **2001**, 97.
- [25] H. Börzel, P. Comba, K. S. Hagen, M. Kerscher, H. Pritzkow, M. Schatz, S. Schindler, O. Walter, *Inorg. Chem.* **2002**, *41*, 5440.
- [26] P. Comba, W. Schiek, *Coord. Chem. Rev.*, in press.
- [27] P. Comba, M. Kerscher, M. Merz, V. Müller, H. Pritzkow, R. Remenyi, W. Schiek, Y. Xiong, *Chem. Eur. J.* **2002**, *8*, 5750.
- [28] P. Comba, S. Kuwata, G. A. Lawrance, *manuscript in preparation*.
- [29] P. Comba, M. Kerscher, A. Roodt, submitted.
- [30] E. A. Ambundo, M.-V. Deydier, A. J. Grall, N. Agnera-Vega, L. T. Dressel, T. H. Cooper, N. J. Heeg, L. A. Ochrymowycz, D. B. Rorabacher, *Inorg. Chem.* **1999**, *38*, 4233.
- [31] D. Wang, G. R. Hanson, *J. Magn. Reson. A* **1995**, *117*, 1.
- [32] D. Wang, G. R. Hanson, *Appl. Magn. Reson.* **1996**, *11*, 401.
- [33] G. M. Sheldrick, SHELXTL NT V5.10, Bruker AXS, Madison, Wisconsin, USA, **1999**.
- [34] C. K. Johnson, ORTEP, *A Thermal Ellipsoid Plotting Program*, Oak National Laboratories, Oak Ridge, TN, **1965**.

Received November 22, 2002